SYNTHESIS AND CHARACTERIZATION OF NANOPARTICLES FROM COAL FLY ASH

Pavel Markov[2], Georgi Chernev[1], Diana Nintianova[3,]
Nadezhda Kazakova[1], Hristo Karakostov[1]

[1]*University of Chemical Technology and Metallurgy*
8 Kliment Ohridski Blvd., Sofia 1797, Bulgaria
[2]*Bulgarian Academy of Sciences*
Institute of General and Inorganic Chemistry
Sofia 1113, Bulgaria
[3]*Bulgarian Academy of Sciences*
Institute of Mineralogy and Crystallography "Akad. Ivan Kostov"
Sofia 1113, Bulgaria
E-mail: g.chernev@uctm.edu

Received 24 July 2023
Accepted 01 September 2024 *DOI: 10.59957/jctm.v59.i6.2024.20*

ABSTRACT

In this study, amorphous nanoparticles were extracted from fly ash using a sol-gel method. The obtained nanoparticles were characterized using XRF spectroscopy, XRD, FT-IR and TEM. The XRD curves show the presence of both crystalline and amorphous phases. FT-IR analysis indicated the presence of silanol and siloxane groups. Upon analysis, the primary nanoparticles were found to exhibit a roughly spherical shape with an average size of approximately 65 nm. The findings of this study demonstrate the feasibility of applying the sol-gel method to synthesize nanoparticles derived from coal fly ash (CFA), thereby avoiding other expensive and energy-intensive methods of nanoparticle synthesis.

Keywords: nanoparticles, fly ash, sol-gel, structure.

INTRODUCTION

Globally, coal remains a significant energy source as indicated by various studies [1 - 4]. Projections suggest that coal will continue to account for 24 % of global electricity production by 2035. However, the historical association of coal combustion with environmental issues such as soil degradation, water and air pollution, and concerns for human health is well-documented [5, 6]. Coal combustion in power plants produces various ash types because of extreme temperatures and pressures [7 - 9]. Coal fly ash (CFA) is collected in electrostatic precipitators and consists mainly of glassy and clay fractions. The coarser ash fraction is collected under boilers in power plants, where it is mixed with water and then transported to pans. CFA is categorized into two main classes, class F and class C, based on the content of Al, Fe and Si oxides, with class F containing a significant amount of silica and class C believed to have a higher calcium content [10]. However, due to its varied structure and physical characteristics, the classification of CFA has become increasingly difficult. The composition of CFA varies depending on the power generation method, boiler type, operating condition, post-combustion technology and coal supply [11 - 14]. CFA has the potential to replace naturally occurring minerals and aggregates in a variety of applications. Silica constitutes between 20 % and 65 % of all fly ash, making the recovery and processing of silica into silicate products a key advantage over historical progress [15]. Several researchers have delved into the extraction of amorphous silica from various materials [16].

The main objective of the present study is the synthesis of CFA nanoparticles using the sol-gel method. The resulting particles were characterized using various structural methods.

Table 1. Chemical composition of CFA by XRF analysis.

Na_2O	MgO	Al_2O_3	SiO_2	P_2O_5	SO_3	Cl	K_2O	CaO	TiO_2	V_2O_5	Cr_2O_3	MnO	Fe_2O_3	NiO	CuO	ZnO
1.03	1.86	19.70	37.30	0.05	3.47	0.01	1.10	6.81	0.76	0.05	0.01	0.09	13.17	0.02	0.32	0.02

EXPERIMENTAL

The CFA components were taken from TPS Bobov dol, Pernik district, Bulgaria. Samples were pretreated using froth flotation to remove unburnt residues. In the process of sample preparation, 50 g of CFA was added to 150 mL of 1 M NaOH solution and heated for 60 min in a water bath with continuous stirring to dissolve the SiO_2 present in CFA and obtain a solution of sodium silicate ($NaSiO_3$). The residue was washed with distilled water and the hot solution was filtered. The filtrate solution was then allowed to cool before being titrated with 1 M HCl to pH 7.5 and left for 24 hours until an aqueous gel formed, which was filtered and dried at 80°C. The resulting dry semi-product is washed repeatedly with warm water and dried at 105°C to constant weight. The structure of synthesized nanomaterials was investigated using following methods:

X-Ray diffraction (XRD) measurements were performed by a Brucker D8 Advance. The diffracted intensity of CuKα radiation was measured with scan rate of 0.020 min^{-1} in 2θ range between 10^0 and 80^0 theta degrees. Infrared Spectra (FT-IR) were obtained using a MATSON 7000 Fourier Transforming Infra-Red spectrometer. Pellets of 2 mg of samples were mixed with 200 mg of spectroscopic grade KBr.

The studies of the microstructure were carried out on a High-Resolution Scanning Transmission electron microscope JEOL JEM 2100, acceleration voltage 80 - 200 kV, maximum resolution 0,23 nm between two points, maximum magnification 1500000x in conventional mode and 2000000x in scanning mode with 5 basic regimes-bright field and dark field microscopy, diffraction from selected and nano-sized area and diffraction in a focused beam. Equipped with CCD camera GATAN Orios 832 SC 1000 and Gatan Microscopy Suit Software Digital Micrograph. The specimen for TEM investigation was prepared by grinding the sample in an agate mortar and then disintegrating it in the form of ethanol suspension by ultrasonic treatment for 6 min. A droplet of the suspension was coated on standard carbon films on Cu grids.

RESULTS AND DISCUSSION

Table 1 displays the results of an XRF study of CFA and nanoparticles. CaO, Al_2O_3, SiO_2, Fe_2O_3, and other trace elements make up the majority of CFA (Table 1).

Structural investigations of the synthesized nanoparticles were carried out. The XRD analysis proved that the nanoparticles are in an amorphous state (Fig. 1). The first diffraction peak can be explained by incomplete hydrolysis of the precursor used, while the second is characteristic of the SiO_2 network [17].

Using FT-IR spectroscopy, results on the structure and presence of functional groups were obtained (Fig. 2). The absorption bands at ~ 3480 cm^{-1} and 1644 cm^{-1} are typical for OH from bound water, as well as from the Si - OH groups. SiO_2 network can be identified with the presence of peaks at around 1080 cm^{-1}, 790 cm^{-1} and 460 cm^{-1}, due to the stretching asymmetric, symmetric and deformation vibrations of the siloxane network. Bands at 950 cm^{-1} and around 560 cm^{-1} are attained to the silanol groups (Si-OH). The lack of bands in the region between 645 cm^{-1} и 720 cm^{-1} is an indication showing that the precursor used for obtaining SiO_2 is completely hydrolyzed. The band at 1637 cm^{-1} refers to the deformation vibration of the absorbed water. Intensive Si-O vibrations at 1007 cm^{-1} suggest the presence of dense SiO_2 structures, where oxygen plays a role of a bridge between the two silica atoms. The band at 1121 cm^{-1} can be explained with the Si-O-Si bond. The shoulder at 570 cm^{-1} can be explained with ν(Si-O) of the silicon dioxide network defects. The band at 690 cm^{-1} is for the νs(Si-O) or plane ν(Si-O^-). Absorption curves at 2973 cm^{-1}, 2887 cm^{-1}, 1468 cm^{-1} and 1257 cm^{-1} are due to stretching and deformation vibration of C - H bands. Peaks at 888, 755 and ~ 670 cm^{-1} indicate presence of Si-C band. Some authors suppose that peaks at 1270 cm^{-1} and ~2970 cm^{-1} prove presence of Si - C band.

The morphology and phase composition of synthesized nanosized materials were investigated using TEM (Figs. 3 and 4). Bright-field images of the studied samples were obtained at different magnifications.

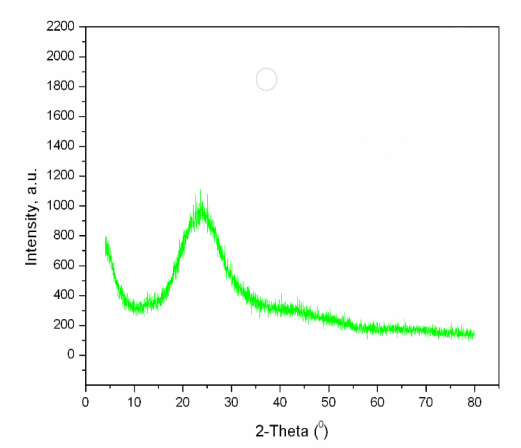

Fig. 1. XRD analysis of silica nanoparticles.

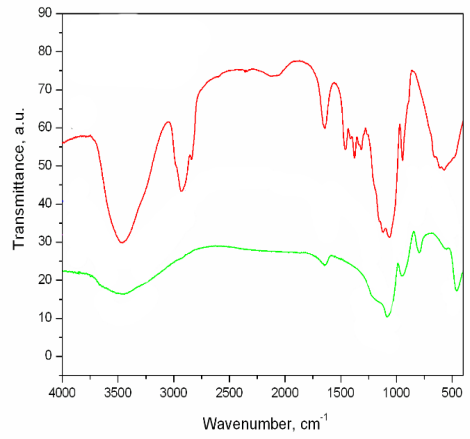

Fig. 2. FT-IR spectra of CFA and nanoparticles.

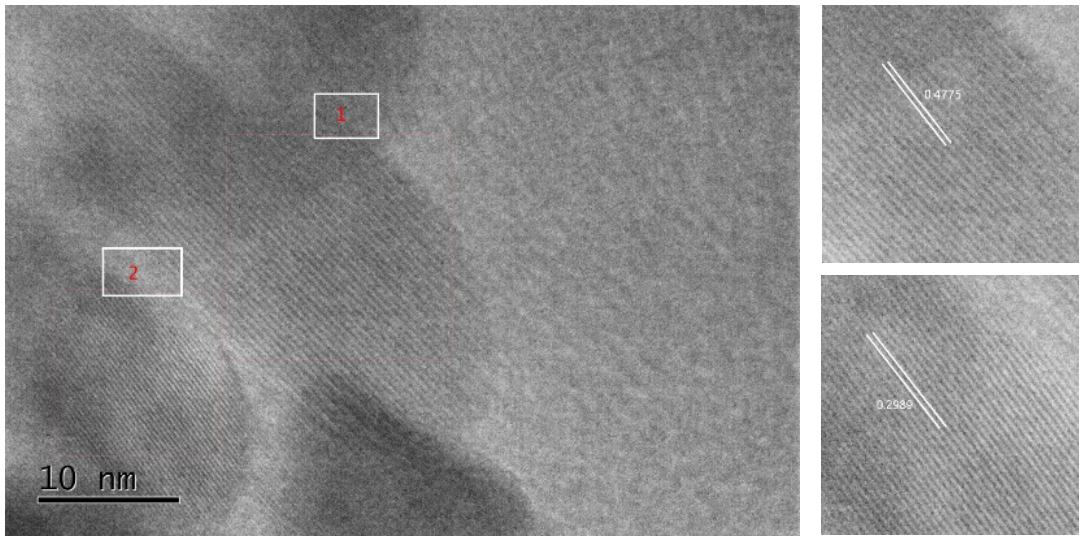

a) b)

Fig. 3. Experimental HRTEM image of synthesized nanoparticles. (a) and Fourier-filtered HRTEM images (b).

High-resolution images (HRTEM) show the presence of tetragonal anatase TiO_2 (89-4203, space group P4/mnm, a = 3.785 Å, c = 9.514 Å) and orthorhombic sillimanite Al_2SiO_5 (space group Pbnm, a = 7.47 Å, b = 7.66 Å, c = 5.75 Å). Traces of hematite, low-temperature quartz, and graphite are also observed. The interplanar distances of the lattice fringes are approximately 0.4775 nm and 0.2989 nm, corresponding to the (002) and (121) planes of the anatase and sillimanite phases, respectively (Fig. 3). The selected area electron diffraction (SAED) reveals the presence of hexagonal Al_2O_3 (51-0769, space group P63/mmc, a = 5.683 Å, c = 22.520 Å) (Fig. 4). Examination of the samples by TEM shows that we have particles of different shapes and sizes - spherical, rectangular, hexagonal [12, 18]. The sizes of the particles are within wide limits, most of them are 10 - 80 nm in size, but there are individual particles with sizes over 200 nm.

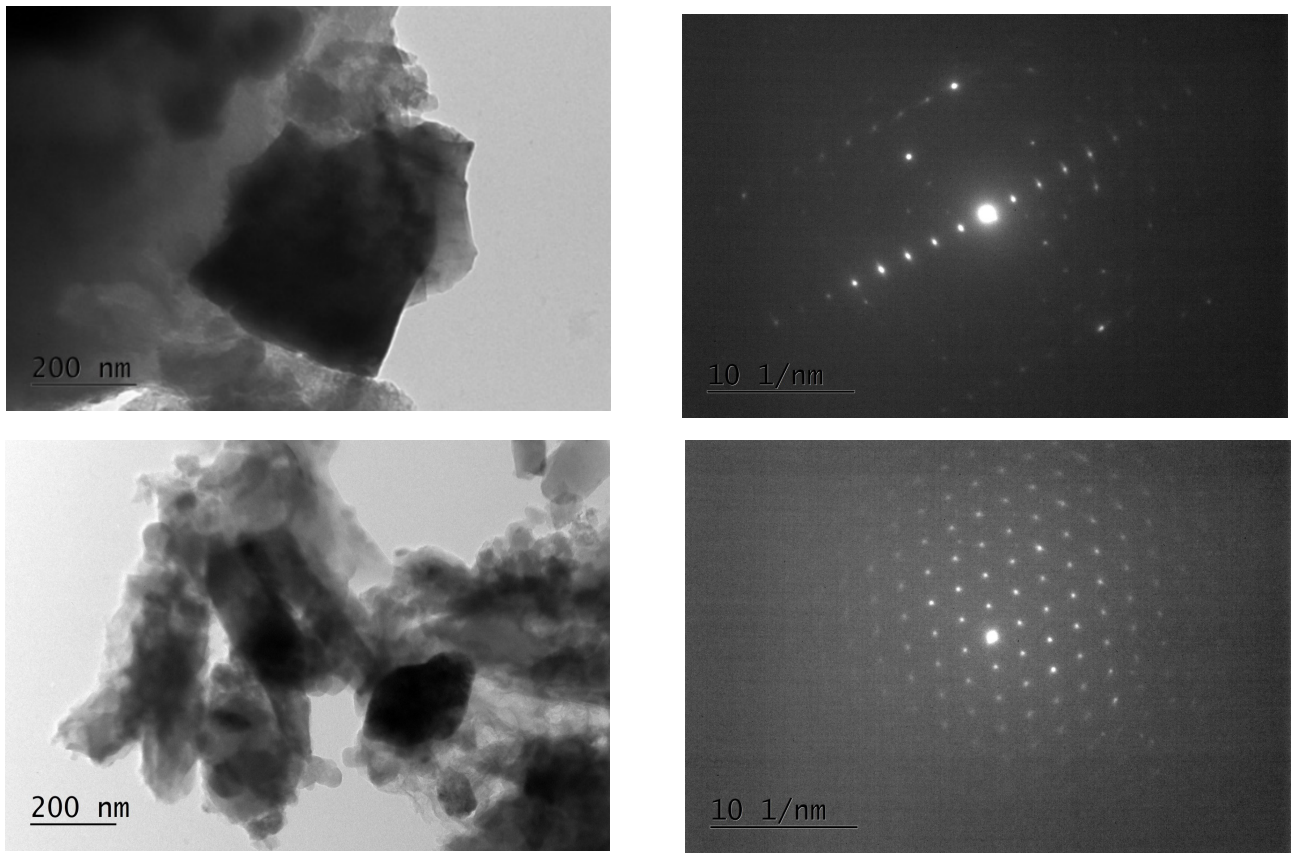

a) b)

Fig. 4. Bright field micrograph (a) and SAED of Al_2O_3 nanosized particle (b).

CONCLUSIONS

Using sol - gel technique, successfully was synthesized nanoparticles with different shapes and size from 10 to 80 nm. XRF analyses confirmed the presence of silica in both FA and the derived silica. Additionally, XRD analysis and FTIR data revealed the primary chemical group in the materials, and the amorphous nature of nanoparticles. TEM investigations show the presence of anatase, silimanite, hematite, Al_2O_3 and traces of low-temperature quartz. This study suggests the potential for further innovation in utilizing fly ash for power thermal station for the preparation of advanced materials with sophisticated applications.

Acknowledgements

This work is developed as part of contract №: BG-RRP-2.004-0002-C01, project BiOrgaMCT, Procedure BG-RRP-2.004 „Establishing of a network of research higher education institutions in Bulgaria", funded by BULGARIAN NATIONAL RECOVERY AND RESILIENCE PLAN. Financial support from Bulgarian Academy of Sciences and Bulgarian Ministry of Education (Project Twinteam D01-272/02.10.2020) is gratefully acknowledged.

REFERENCES

1. Q. Liu, M. Sun, X. Sun, B. Liu, M. Ostadhassan, W. Huang, X. Chen, Z. Pan, Pore network characterization of shale reservoirs through state-of-the-art X-ray computed tomography: A review, Gas Science and Engineering, 113, 2023, 204967.
2. P. Jia, S. Nadimi, J. Jia, Quantitative micromechanical and pore structural characterization of coal before and after freezing, Fuel, 16, 2022, 123421.
3. B. Demirbağ, B. Bayrak, Ç. Gamze Özkan, E.

Çaylak, Evaluation of the Life Quality of Workers in a Cement Factory, Procedia - Social and Behavioral Sciences, 237, 2017, 1462-1467.
4. L. Suna, Z. Wang, B. Gao, Ceramic membranes originated from cost-effective and abundant natural minerals and industrial wastes for broad applications - a review, Desalination and Water Treatment, 201, 2020, 121-138.
5. K. Priyam Goswami, K. Pakshirajan, G. Pugazhenthi, Process intensification through waste fly ash conversion and application as ceramic membranes: A review, Science of The Total Environment, 808, 2022, 151968.
6. Y. Niu, S. Liu, B. Yan, Sh. Wang, X. Zhang, Sh. Hui, Effects of CO_2 gasification reaction on the combustion of pulverized coal char, Fuel, 233, 2018, 77-83.
7. A. Reynolds, T. Verheyen, S. Adeloju, A. Chaffee, E. Meuleman, Monoethanolamine degradation during pilot-scale post-combustion capture of CO_2 from a brown coal-fired power station, Energy Fuels, 29, 2015, 7441-7455.
8. A. Creamer, B. Gao, Carbon-based adsorbents for post-combustion CO_2 capture: a critical review, Environ. Sci. Technol., 50 2016, 7276-7289.
9. M. Maroto-Valer, Z. Lu, Y. Zhang, Z. Tang, Sorbents for CO_2 capture from high carbon fly ashes. Waste Manag. 28, 2008, 2320-2328.
10. D.K. Nayak, P.P. Abhilash, R. Singh, R. Kumar, V. Kumar, Fly ash for sustainable construction: A review of fly ash concrete and its beneficial use case studies, Cleaner Materials, 6, 2022, 100143.
11. T.H. Liou, C.C. Yang, Synthesis and surface characteristics of nanosilica produced from alkali extracted rice husk ash, Mater. Sci. Eng. B, 176, 2011, 521-529.
12. V. Ivanova, Y. Trifonova, V. Lilova, V. Mikli, A. Stoyanova-Ivanova, Structural investigation of tellurium based thin films, J. Chem. Technol. Metall., 53, 4, 2018, 749-754.
13. V. Carmona, R. Oliveira, W. Silva, L. Mattoso, J. Marconcini, Nanosilica from rice husk: extraction and characterization, Ind. Crops Prod., 43, 2013, 291-296.
14. J.K. Tishmack, P.E. Burns, The chemistry and mineralogy of coal and coal combustion products, Geological Society London 236, 1, 2004, 223-246.
15. V. Kumar Yadav, M.H. Fulekar, Advances in Methods for Recovery of Ferrous, Alumina, and Silica Nanoparticles from Fly Ash Waste, Ceramics, 3, 3, 2020, 384-420.
16. P.U. Nzereogu, A.D. Omah, F.I. Ezema, E.I. Iwuoha, A.C. Nwanya, Silica extraction from rice husk: Comprehensive review and applications, Hybrid Advances, 4, 2023, 100111.
17. I. Karadashka, V. Ivanova, V. Jordanov, V. Karadjova Glass Formation and Properties of Multicomponent Glasses of the As_2Se_3-Ag_2Te-GeTe System, Inorganics, 12, 1, 2024, 11.
18. A. Stoilova, V. Lilova, V. Ivanova, Y. Trifonova, D. Dimov, Optical properties of electrospray deposited pazo polymer films doped with $GeTe_4$ -Cu chalcogenide particles, J. Chem. Technol. Metall., 57, 1, 2022, 126-131.